Catal Lett (2008) 123:90–95
DOI 10.1007/s10562-008-9399-3

Chemical Immobilization of $H_5PMo_{10}V_2O_{40}$ ($PMo_{10}V_2$) Catalyst on Nitrogen-rich Macroporous Carbon (N-MC) for Use as an Oxidation Catalyst

Joohyung Lee · Heesoo Kim · Kyung Won La · Dong Ryul Park · Ji Chul Jung · Sang Hee Lee · In Kyu Song

Received: 10 December 2007 / Accepted: 9 January 2008 / Published online: 24 January 2008

Abstract Nitrogen-rich macroporous carbon (N-MC) was prepared using melamine-formaldehyde resin as a carbon precursor. The surface of N-MC was then modified to have a nitrogen-derived functional group (amine group), and thus, to provide an anchoring site for heteropolyacid (HPA) catalyst. By taking advantage of the overall negative charge of $[PMo_{10}V_2O_{40}]^{5-}$, $H_5PMo_{10}V_2O_{40}$ ($PMo_{10}V_2$) HPA catalyst was chemically immobilized on the N-MC support as a charge matching component. It was found that $PMo_{10}V_2$ was finely dispersed on the N-MC support. In the model vapor-phase 2-propanol conversion reaction, the $PMo_{10}V_2$/N-MC catalyst showed a remarkably enhanced oxidation catalytic activity and a suppressed acid catalytic activity compared to the mother catalyst. The $PMo_{10}V_2$/N-MC catalyst served as an efficient oxidation catalyst in the reaction where both acid and oxidation reactions occurred simultaneously.

Keywords Heteropolyacid catalyst · Macroporous carbon · Chemical immobilization · Oxidation catalysis

1 Introduction

Heteropolyacids (HPAs) are early transition metal-oxygen anion clusters that exhibit a wide range of molecular sizes, compositions, and molecular architectures [1]. Among various HPA structural classes, the Keggin-type HPAs have been widely employed as homogeneous and heterogeneous catalysts for acid–base and oxidation reactions [2, 3]. A great advantage of HPA catalysts is that their catalytic properties can be tuned in a systematic way by changing the identity of counter-cation, heteroatom, and framework polyatom [4]. Their excellent thermal and chemical stabilities also make them good candidates in catalytic applications that may require harsh environments [5]. However, a disadvantage of HPA catalysts is that their surface area is very low (<10 m^2/g). To overcome the low surface area, HPAs have been supported on inorganic materials by a conventional impregnation method [6–9]. Another promising approach for enlarging the surface area of HPA catalysts is to take advantage of the overall negative charge of heteropolyanion. By this method, HPA catalysts have been immobilized on the positively charged polymer materials [10, 11]. Although such an attempt utilizing inorganic materials has been restricted due to the difficulty in forming a positive charge on the inorganic materials, HPA catalysts have been successfully immobilized on the inorganic supporting materials such as mesoporous carbon [12] and mesostructured cellular foam silica [13].

Among various inorganic supporting materials, porous carbons have attracted much attention as supporting materials due to their excellent thermal stability and unique textural property [14, 15]. Porous carbons have been widely prepared using sucrose [16, 17], polydivinylbenzene [18, 19], furfuryl alcohol [20], and phenolic resin [21] as a carbon precursor. If a porous carbon is modified to have a positive charge, it can serve as an excellent supporting material for HPA catalyst. Although a porous carbon with a nitrogen-derived positive functional group has been developed from a nitrogen-free porous carbon [12], it was found to have a limited number of positive anchoring sites for the chemical immobilization of HPA catalyst. This is because the formation of nitrogen-derived

J. Lee · H. Kim · K. W. La · D. R. Park · J. C. Jung · S. H. Lee · I. K. Song (✉)
School of Chemical and Biological Engineering, Seoul National University, Shinlim-dong, Kwanak-ku, Seoul 151–744, South Korea
e-mail: inksong@snu.ac.kr

anchoring sites on the nitrogen-free porous carbon is essentially restricted due to the hydrophobic nature and chemical inertness of carbon material. The process for obtaining a positively charged porous carbon from a nitrogen-free porous carbon also requires many treatment steps. If a nitrogen-containing porous carbon is prepared by a single step, therefore, it can be easily modified to have a nitrogen-derived functional group for the chemical immobilization of HPA catalyst.

In this work, nitrogen-rich macroporous carbon (N-MC) was prepared for use as a support for HPA catalyst. Melamine-formaldehyde resin was used as a carbon precursor, with an aim of increasing nitrogen content on the N-MC. The surface of N-MC was then modified to have a positive charge, and thus, to provide a site for the chemical immobilization of HPA catalyst. The Keggin-type $H_5PMo_{10}V_2O_{40}$ ($PMo_{10}V_2$) catalyst was immobilized on the surface-modified N-MC support, by taking advantage of the overall negative charge of $[PMo_{10}V_2O_{40}]^{5-}$. The $PMo_{10}V_2$ catalyst immobilized on the N-MC support ($PMo_{10}V_2$/N-MC) was applied to the model vapor-phase 2-propanol conversion reaction to explore the oxidation catalytic activity of $PMo_{10}V_2$/N-MC.

2 Experimental

2.1 Preparation of $PMo_{10}V_2$/N-MC Catalyst

Figure 1 shows the schematic procedures for the preparation of $PMo_{10}V_2$/N-MC catalyst. Silica sphere with a diameter of ca. 300 nm was synthesized according to the method in the literature [22]. A precursor mixture with a weight ratio of melamine (>99.5 wt%):formaldehyde (35 wt%):ammonia (36 wt%) = 1.0:1.8:0.1 was prepared at room temperature under vigorous stirring. After adding silica sphere to the mixture, it was polymerized at 80 °C for 12 h. The polymer-silica composite was then carbonized at 900 °C for 4 h at a heating rate of 5 °C/min in a stream of nitrogen. After carbonization, silica sphere was removed using an aqueous HF(48 wt%) solution. After filtering and washing the resulting solid with deionized water, it was dried at 70 °C for 12 h to yield the nitrogen-rich macroporous carbon (N-MC).

The surface of N-MC was activated with a stream of hydrogen at 200 °C for 2 h to form an amine functional group. The activated N-MC was then treated with an aqueous HCl solution for 12 h to have a positive charge. Surface-modified N-MC (1.0 g) and $PMo_{10}V_2$ catalyst (1.0 g) were added to acetonitrile (100 mL), and the slurry was stirred at room temperature for 24 h for the chemical immobilization of $PMo_{10}V_2$ on the amine functional group of N-MC. The resulting slurry was filtered and washed with deionized water several times, until the washing solvent became colorless. The solid product was dried at 80 °C overnight in a convection oven, and then it was finally calcined at 300 °C for 2 h to yield the $PMo_{10}V_2$/N-MC catalyst.

2.2 Characterization

Nitrogen adsorption–desorption isotherms were obtained using a Micromeritics ASAP-2010 instrument. Surface

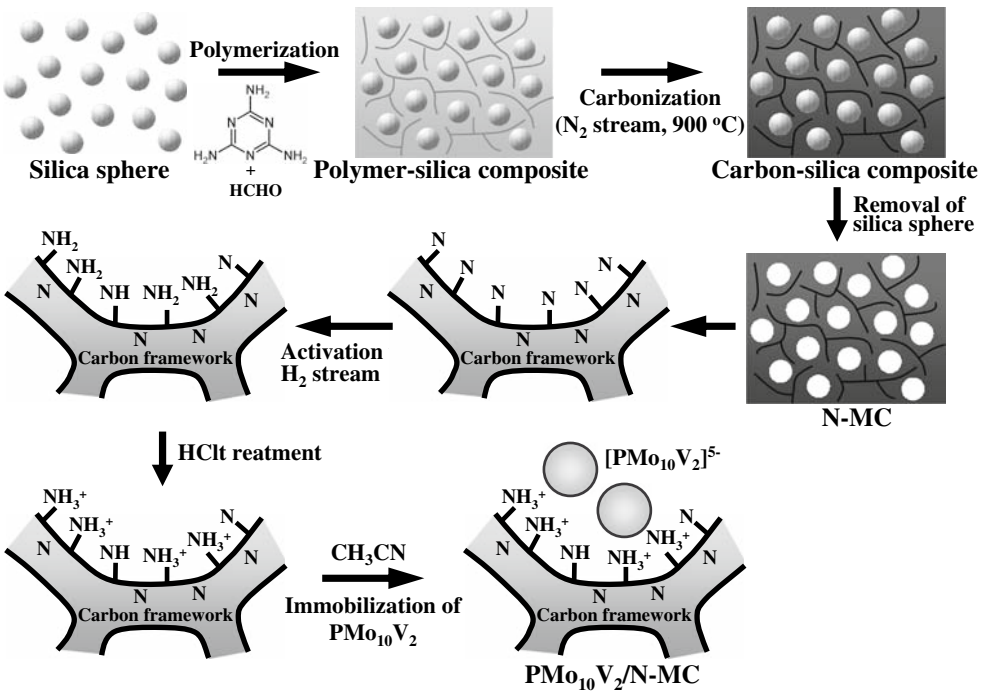

Fig. 1 Schematic procedures for the preparation of $PMo_{10}V_2$/N-MC catalyst

area was calculated using the Brunauer-Emmett-Teller (BET) method. Pore volume was calculated using the Barrett-Joyner-Halenda (BJH) method. CHN elemental analyses were conducted with a LECO CHNS-932 analyzer. FE-SEM images were obtained with a JEOL JSM-6700F microscope. TEM images were obtained with a JEOL JEM-3010 microscope operated at 300 kV. FT-IR spectra were obtained with a Nicolet Magna-IR 750 spectrometer. ^{31}P CP-MAS NMR spectra were measured at room temperature with a Bruker Avance 400WB spectrometer (spectrometer frequency = 162.0849 MHz, spin rate = 8 kHz). XRD patterns were obtained with a MAC Science M18XHF instrument using Cu Kα radiation.

2.3 Vapor-Phase 2-Propanol Conversion Reaction

Oxidation catalytic activity of $PMo_{10}V_2$/N-MC catalyst was investigated by performing the model vapor-phase 2-propanol conversion reaction. The reaction was carried out in a continuous flow fixed-bed reactor at atmosphere pressure. Either supported or unsupported catalyst (60 mg on $PMo_{10}V_2$ basis) was charged into a tubular quartz reactor, and then it was pretreated with a mixed stream of nitrogen (10 mL/min) and oxygen (5 mL/min) at 220 °C for 2 h. The reaction temperature was maintained at 180 °C. 2-Propanol (1.3×10^{-2} mol/h) was sufficiently vaporized and was fed into the reactor together with a mixed stream of nitrogen (10 mL/min) and oxygen (5 mL/min). Reaction products were periodically sampled and analyzed with a gas chromatograph (HP 5890II).

3 Results and Discussion

3.1 Characterization of N-MC and $PMo_{10}V_2$/N-MC

Figure 2 shows the nitrogen adsorption–desorption isotherms of N-MC support and $PMo_{10}V_2$/N-MC catalyst. Both N-MC and $PMo_{10}V_2$/N-MC exhibited the type-IV isotherms and type-H3 hysteresis loops with no great difference. Chemical compositions and physical properties of N-MC and $PMo_{10}V_2$/N-MC are summarized in Table 1. BET surface area and pore volume of N-MC were 643 m^2/g and 0.86 cm^3/g, respectively. Even after the immobilization of $PMo_{10}V_2$ on N-MC, $PMo_{10}V_2$/N-MC catalyst still retained high surface area (590 m^2/g) and large pore volume (0.80 cm^3/g). CHN elemental analyses revealed that nitrogen content in the N-MC was 10.6 wt%, while that in the $PMo_{10}V_2$/N-MC was measured to be 8.4 wt%. The decreased nitrogen content of $PMo_{10}V_2$/N-MC was due to the loading of $PMo_{10}V_2$. $PMo_{10}V_2$ loading in the $PMo_{10}V_2$/N-MC catalyst determined by ICP elemental analysis was

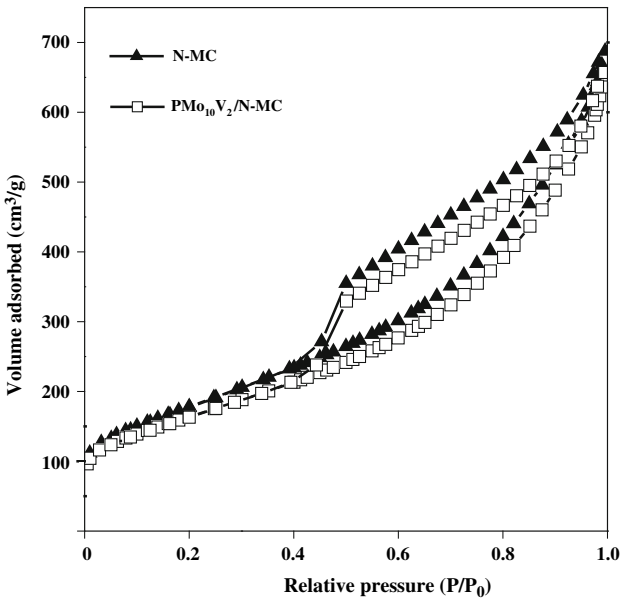

Fig. 2 Nitrogen adsorption–desorption isotherms of N-MC and $PMo_{10}V_2$/N-MC

7.6 wt%. It is interesting to note that $PMo_{10}V_2$ catalyst supported on N-MC by a conventional impregnation method was totally dissolved out during the washing step with deionized water. This indicates that the nitrogen-derived functional group (amine group) of surface-modified N-MC played a key role for the immobilization of $PMo_{10}V_2$.

Figure 3 shows the FE-SEM and TEM images of N-MC. The images clearly show the formation of macropores with an average pore size of ca. 300 nm. Surface morphology of N-MC was almost identical to that of $PMo_{10}V_2$/N-MC. This indicates that macropore structure of N-MC was still maintained even after the immobilization of $PMo_{10}V_2$ catalyst.

3.2 Chemical Immobilization of $PMo_{10}V_2$ on the N-MC Support

Chemical immobilization of $PMo_{10}V_2$ on the N-MC support was well confirmed by FT-IR and ^{31}P CP-MAS NMR analyses. Figure 4 shows the FT-IR spectra of N-MC, $PMo_{10}V_2$, and $PMo_{10}V_2$/N-MC. The primary structure of $PMo_{10}V_2$ could be identified by the four characteristic IR bands appearing in the range of 700–1,100 cm^{-1}. The

Table 1 Chemical compositions and physical properties of N-MC and $Pmo_{10}V_2$/N-MC

Sample	Nitrogen content (wt%)	$Pmo_{10}v_2$ content (wt%)	BET suface area (m^2/g)	BJH pore volume (cm^3/g)
N-MC	10.6	–	643	0.86
$Pmo_{10}V_2$/N-MC	8.4	7.6	590	0.80

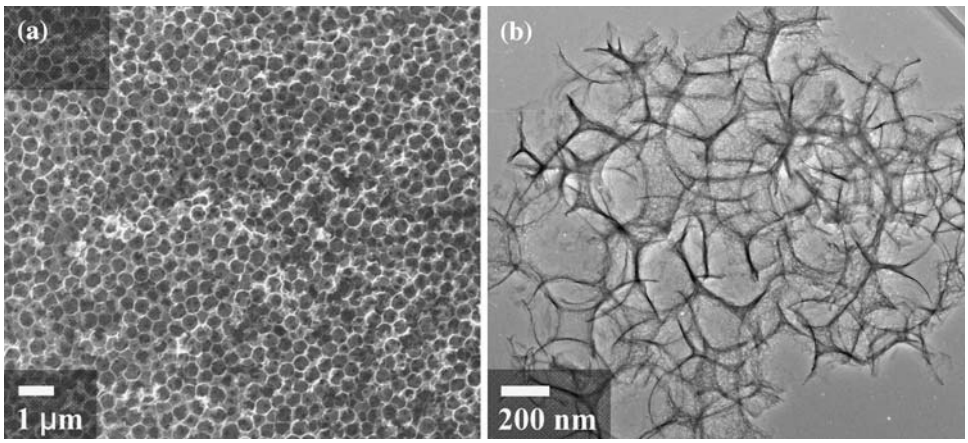

Fig. 3 (**a**) FE-SEM and (**b**) TEM images of N-MC

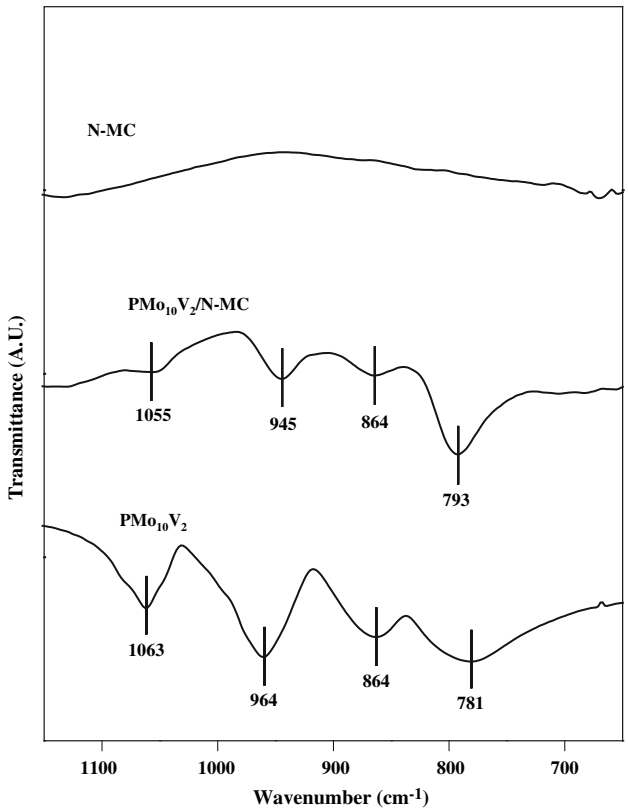

Fig. 4 FT-IR spectra of N-MC, $PMo_{10}V_2$, and $PMo_{10}V_2$/N-MC

four characteristic IR bands of unsupported $PMo_{10}V_2$ appeared at 1,063 cm^{-1} (P–O), 964 cm^{-1} (M(polyatom)=O), 864 cm^{-1} (interoctahedral M–O–M), and 781 cm^{-1} (intraoctahedral M–O–M). On the other hand, no characteristic IR bands of N-MC were observed in the range of 700–1,100 cm^{-1} due to the strong absorbance of carbon material by infrared beam. The characteristic IR bands of $PMo_{10}V_2$/N-MC appeared at 1,055 cm^{-1} (P–O), 945 cm^{-1} (M=O), 864 cm^{-1} (interoctahedral M–O–M), and 793 cm^{-1} (intraoctahedral M–O–M). In other words, the characteristic IR bands of $PMo_{10}V_2$ in the $PMo_{10}V_2$/N-MC appeared at slightly shifted positions compared to those of unsupported $PMo_{10}V_2$. This indicates that $PMo_{10}V_2$ was successfully immobilized on the N-MC support via strong chemical interaction between two components.

Figure 5 shows the ^{31}P CP-MAS NMR spectra of $PMo_{10}V_2$ and $PMo_{10}V_2$/N-MC. Unsupported $PMo_{10}V_2$ showed a chemical shift at $\delta = -3.9$ ppm, while $PMo_{10}V_2$/N-MC showed a chemical shift at $\delta = -6.3$ ppm. It is believed that the difference in chemical shift of structural phosphorous between $PMo_{10}V_2$ and $PMo_{10}V_2$/N-MC was attributed to the strong chemical interaction between $PMo_{10}V_2$ and N-MC.

3.3 Fine Dispersion of $PMo_{10}V_2$ on the N-MC Support

Fine dispersion of $PMo_{10}V_2$ on the N-MC support was confirmed by XRD analyses. Figure 6 shows the XRD patterns of N-MC, $PMo_{10}V_2$, and $PMo_{10}V_2$/N-MC. Unsupported $PMo_{10}V_2$ showed the characteristic XRD peaks of the

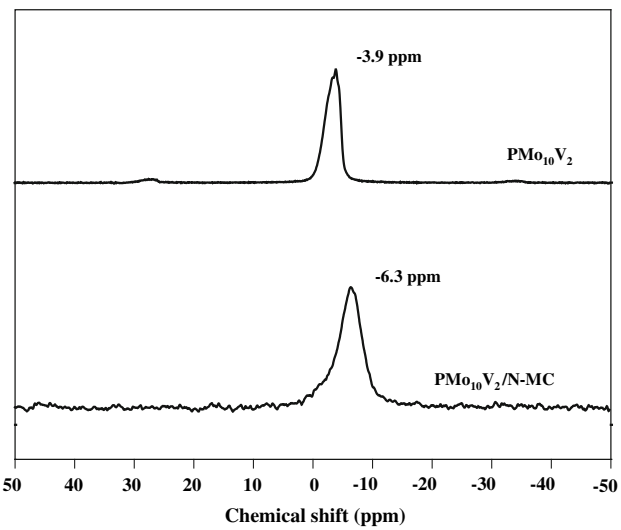

Fig. 5 ^{31}P CP-MAS NMR spectra of $PMo_{10}V_2$ and $PMo_{10}V_2$/N-MC

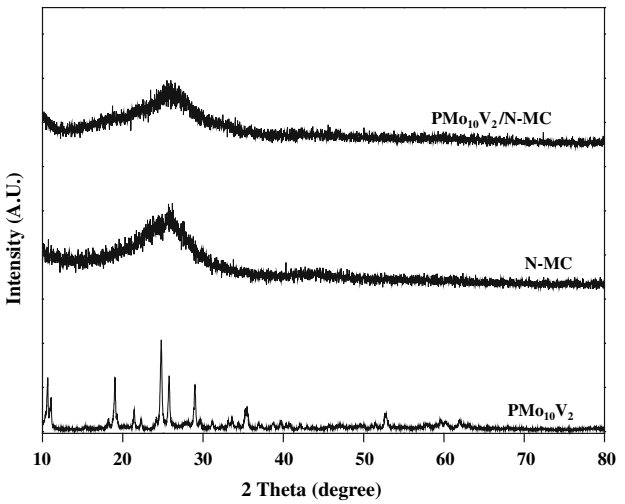

Fig. 6 XRD patterns of N-MC, $PMo_{10}V_2$, and $PMo_{10}V_2$/N-MC

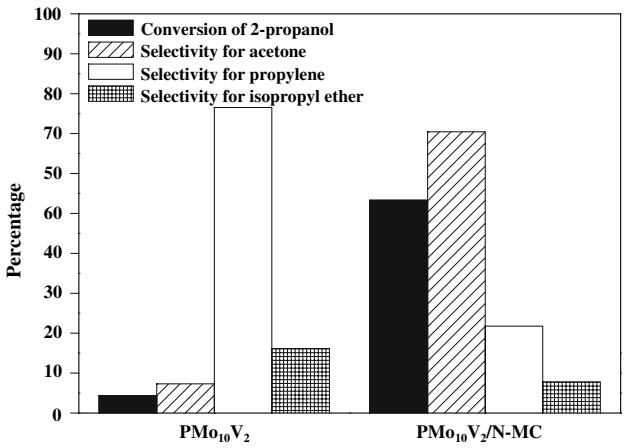

Fig. 7 Catalytic activity of $PMo_{10}V_2$ and $PMo_{10}V_2$/N-MC catalysts in the vapor-phase 2-propanol conversion reaction at 180 °C after a 6 h-reaction

HPA. However, N-MC showed no characteristic XRD pattern due to its amorphous nature. Interestingly, $PMo_{10}V_2$/N-MC also showed the same amorphous XRD pattern as N-MC. This indicates that $PMo_{10}V_2$ was not in crystal state but in an amorphous-like state on the N-MC support. The above result strongly supports that $PMo_{10}V_2$ was finely and molecularly dispersed on the N-MC in the $PMo_{10}V_2$/N-MC catalyst.

3.4 Catalytic Performance in the 2-Propanol Conversion Reaction

Figure 7 shows the typical catalytic performance of $PMo_{10}V_2$ and $PMo_{10}V_2$/N-MC catalysts in the vapor-phase 2-propanol conversion reaction at 180 °C after a 6 h-reaction. It is known that propylene and isopropyl ether are formed by the acid catalysis of HPA, while acetone is produced by the oxidation catalysis of HPA [23]. As shown in Fig. 7, the $PMo_{10}V_2$/N-MC catalyst showed a higher 2-propanol conversion than the $PMo_{10}V_2$ catalyst. Furthermore, the $PMo_{10}V_2$/N-MC catalyst showed an enhanced oxidation catalytic activity (formation of acetone) and a suppressed acid catalytic activity (formation of propylene and isopropyl ether) compared to the $PMo_{10}V_2$ catalyst. The remarkably enhanced 2-propanol conversion over $PMo_{10}V_2$/N-MC catalyst was due to the fine dispersion of $[PMo_{10}V_2O_{40}]^{5-}$ on the N-MC support formed via chemical immobilization. As attempted in this work, it is believed that $[PMo_{10}V_2O_{40}]^{5-}$ was chemically and strongly immobilized on the N-MC support as a charge-matching component by losing the proton (Brönsted acid site) of $PMo_{10}V_2$. Therefore, the $PMo_{10}V_2$/N-MC catalyst showed an enhanced oxidation catalytic activity and a suppressed acid catalytic activity compared to the mother catalyst.

4 Conclusions

Nitrogen-rich macroporous carbon (N-MC) was prepared by a templating method using melamine-formaldehyde resin and silica sphere as a carbon precursor and a template, respectively, for use as a support for HPA catalyst. The $H_5PMo_{10}V_2O_{40}$ ($PMo_{10}V_2$) catalyst was successfully immobilized on the surface-modified N-MC support by taking advantage of the overall negative charge of $[PMo_{10}V_2O_{40}]^{5-}$. The nitrogen-derived functional group (amine group) of N-MC played a key role for the chemical immobilization of $PMo_{10}V_2$. It was revealed that $PMo_{10}V_2$ was finely immobilized on the N-MC support via strong chemical interaction between two components. In the model vapor-phase 2-propanol conversion reaction, the $PMo_{10}V_2$/N-MC catalyst showed a higher 2-propanol conversion and a better oxidation catalytic activity than the mother catalyst. The remarkably enhanced oxidation catalytic activity of $PMo_{10}V_2$/N-MC was due to the fine dispersion of $[PMo_{10}V_2O_{40}]^{5-}$ on the N-MC support formed via chemical immobilization by sacrificing the proton of $PMo_{10}V_2$. Thus, the $PMo_{10}V_2$/N-MC served as a selective oxidation catalyst in the model reaction where both acid and oxidation reactions occurred simultaneously.

Acknowledgments The authors wish to acknowledge support from the Seoul Renewable Energy Research Consortium (Seoul R & BD Program) and RCECS (Research Center for Energy Conversion and Storage: R11-2002-102-00000-0).

References

1. Misono M (1987) Catal Rev Sci Eng 29:269
2. Hill CL, Prosser-McCartha CM (1995) Coord Chem Rev 143:407
3. Mizuno N, Misono M (1998) Chem Rev 98:199
4. Okuhara T, Mizuno N, Misono M (1996) Adv Catal 41:113

5. Pope MT (1983) Heteropoly and isopoly oxometalates. Springer-Verlag, New York
6. Damyanova S, Dimitrov L, Mariscal R, Fierro JLG, Petrov L, Sobrados I (2003) Appl Catal A 256:183
7. Kozhevnikov IV (1995) Catal Lett 30:241
8. Chu W, Yang X, Shan Y, Ye X, Wu Y (1996) Catal Lett 42:201
9. He N-Y, Woo C-S, Kim H-G, Lee H-I (2005) Appl Catal A 281:167
10. Hasik M, Poźniczek J, Piwowarska Z, Dziembaj R, Bielański A, Proń A (1994) J Mol Catal 89:329
11. Poźniczek J, Kulszewicz-Bajer I, Zagórska M, Kruczała K, Dyrek K, Bielański A, Proń A (1991) J Catal 132:311
12. Kim H, Kim P, Lee K-Y, Yeom SH, Yi J, Song IK (2006) Catal Today 111:361
13. Kim H, Jung JC, Kim P, Yeom SH, Lee K-Y, Song IK (2006) J Mol Catal A 259:150
14. Marsh H, Heintz EA, Rodriguez-Reinoso F (1997) Introduction to carbon technology. Universidad de Alicante, Secretariado de Publications, Alicante, Spain
15. Patrick JW (1995) Porosity in carbons: characterization and applications. Edward Arnold, London
16. Jun S, Joo SH, Ryoo R, Kruk M, Jaroniec M, Liu Z, Ohsuna T, Terasaki O (2002) J Am Chem Soc 122:10712
17. Solovyov LA, Zaikovskii VI, Shamakov AN, Belousov OV, Ryoo R (2002) J Phys Chem B 106:12198
18. Moriguchi I, Koga Y, Matsukura R, Teraoka Y, Kodama M (2002) Chem Commun 1844
19. Yoon SB, Kim JY, Yu J-S (2001) Chem Commun 559
20. Che S, Lund K, Tatsumi T, Iijima S, Joo SH, Ryoo R, Terasaki O (2003) Angew Chem Int Ed 115:2232
21. Yu J-S, Kang S, Yoon SB, Chai G (2002) J Am Chem Soc 124:9382
22. Stöber W, Fink A, Bohn E (1968) J Coll Inter Sci 26:62
23. Lee JK, Song IK, Lee WY, Kim J-J (1996) J Mol Catal A 104:311